

Effect Change Concrete Slab Layer Thickness on Rigid Pavement

G. A. Almashhadani

Department of Civil Engineering
University of Baghdad
Baghdad, Iraq

G.Almashhadani1901M@coeng.uobaghdad.edu.iq

Mohannad H. Al-Sherrawi

Department of Civil Engineering
University of Baghdad
Baghdad, Iraq

dr.mohannad.alsherrawi@coeng.uobaghdad.edu.iq

Received: 23 August 2022 | Revised: 16 September 2022 and 25 September 2022 | Accepted: 26 September 2022

Abstract—Years of research have been devoted to developing a tool to model and analyze the behavior of rigid pavements. A major component of the new design approaches is the three-dimensional Finite Element Method (FEM), which caused a breakthrough in rigid pavement analysis. The current study used FEM to analyze a rigid pavement composed of a concrete slab layer and a subgrade. The impact of the depth of the concrete slab layer on vertical stresses and displacements was studied with the ABAQUS software. Three different thicknesses were chosen, 20, 25, and 28cm, while the thickness of the remaining paving layers remained unchanged. According to the study results, the top of the concrete slab layer had an increase in stress of approximately 88% when its thickness increased from 20 to 28cm, whereas the top of the subgrade layer had a decrease of about 21% in stress. The change in vertical stress at the top of the subgrade layer was 46% for a thickness of 20-25cm and 14.8% for 25-28cm. The percent of the reduction in vertical stress at the top of the concrete slab layer was 13.2% and 1.8% for thicknesses of 20-25 and 25-28cm respectively. Vertical displacement in the middle of the horizontal distance under the tire print was reduced by 14%, 12%, and 24% when the concrete slab layer increased from 20 to 25, from 25 to 28, and from 20 to 28cm respectively.

Keywords—rigid pavement; ABAQUS; concrete slab thickness; finite element method

I. INTRODUCTION

Rigid pavements are complicated structural systems made up of a variety of concrete slabs connected by longitudinal and transverse joints that may or may not contain dowel bars. Many design approaches to determine required pavement thicknesses have been established [1]. Analytical solutions developed from closed-form formulas to complicated derivations can be used to determine stress and strain on rigid pavements. Finite Element (FE) modeling is useful to simulate the structural reaction of pavements under the influence of various loading conditions and is effective in solving partial and integral differential equations [2-4]. FEM was developed as a numerical approach to solve numerous engineering and applied science issues [5]. Many techniques with various computational costs may be implemented in ABAQUS, a software widely used for FEM analysis [6], as it can solve problems with static, harmonic, and

transient dynamic loading as well as thermal gradient conditions in two and three dimensions [7]. Linear and nonlinear elastic, viscoelastic, plastic, and modified elastic materials can be represented.

Several studies used three-dimensional (3D) FE models to investigate the behavior of rigid pavements. Various FE models have been proposed to analyze the behavior of concrete pavement systems. In [8], the tension in rigid runway pavement was studied showing that wider wheel arrangements cause less stress by aircraft load. Computational modeling of a rigid pavement with load applied to the slab's edge was conducted in [1] using FEM. There were no significant variations in stresses at the research control point between modeling a system with three slabs with dowels and modeling an isolated slab for slab sizes frequently used in basic concrete pavements ($L \geq 3.5m$). An analysis of a dowel-jointed concrete pavement using a 3D FE model was carried out in [9], observing that voids beneath the joint increased the vertical displacement of the concrete slab and vertical stress at the concrete/dowel bar interface, potentially leading to concrete crushing and dowel loosening. In [2], ABAQUS was used to investigate the pavement response under the effect of some model parameters, and a comparison with field measurements confirmed the findings. The stress and strains on the concrete slabs were found to minimize by increasing the thickness of the slab. Stress reduction is especially noticeable in the joints. In [11], ABAQUS was employed to model rigid pavements and investigate how varied pavement layer thicknesses, such as base course material and slab thickness, affected the critical pavement reactions.

II. MATERIALS AND METHODS

A. Pavement Model

This study modeled the concrete slab and subgrade using a 3D FE mesh. A conventional pavement section was used, consisting of a concrete slab and a subgrade, to investigate the effect of the thickness of the concrete slab layer on the performance of the rigid pavement layers, with a fixed subgrade depth thickness. The geometries and the mechanical properties of the materials examined were the elastic modulus E and Poisson's ratio ν . The data of the adopted model were:

Corresponding author: Ghfran A. Almashhadani

- Concrete slab layer of 4.50×5.00m, $h=200\text{mm}$
- $E_c=26000\text{MPa}$, $\nu=0.17$
- Subgrade of 4.50×5.00m, $h=3.00\text{m}$.
- $E=34\text{MPa}$, $\nu=0.35$

Figure 1 shows the geometrical model.

TABLE I. LAYER THICKNESSES

Layer	Layer name	Thickness		
		Case 1	Case 2	Case 3
1	Concrete slab	180 mm	200 mm	250 mm
2	Subgrade	3 m	3 m	3 m

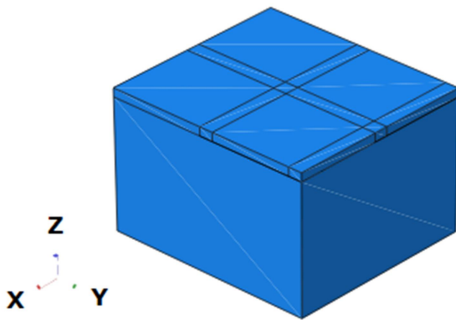


Fig. 1. 3-D model, geometry.

B. Mesh Size Distribution in the Model

The mesh size was optimized to achieve a balance between computation time and calculation stability [4]. A fine mesh of 10×10cm was required in the concrete slab. However, a somewhat coarse mesh of 30×30cm was chosen for the soil foundation, without affecting the accuracy of the stress and displacement predictions. Figure 2 shows the model's FE mesh.

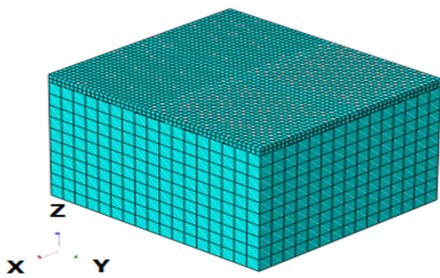


Fig. 2. Mesh size distribution for the model.

C. Boundary Conditions

The boundary conditions were chosen to be as close as possible to the actual boundary conditions. The peripheric and bottom limitations were defined using the boundary conditions. For boundary conditions, the lower surfaces were considered completely fixed against all degrees of freedom [10]. For all pavement geometry models, the edges can move in the vertical (z) direction. No movement was considered in the horizontal directions for the four sides of the model during FEM analysis. Figure 3 shows these boundary conditions.

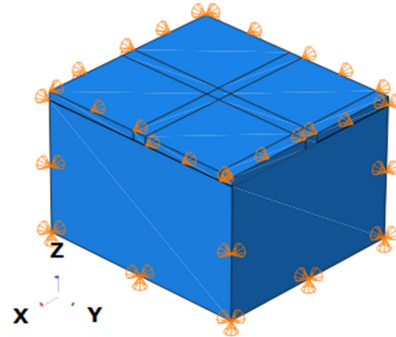


Fig. 3. The boundary conditions of the model.

D. Load Representation

The load was characterized as static, which is the most favorable state for calculating stresses, and the equivalent contact area was used in the load configuration, which is a common technique of representing pavement loads [3]. The single axle, with a single wheel, and a 690kPa pressure of the tire was adopted in the analysis. The use of a square footprint resulted in an improved agreement with FE meshing. Figure 4 shows the wheel load configurations, and Table II presents footprint dimensions.

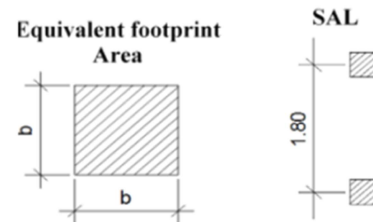


Fig. 4. Wheel load configurations.

TABLE II. FOOTPRINT DIMENSIONS [3]

Wheel load	Dimensions "b" (mm)
Single wheel load (SAL)	332

E. Interaction Modeling Techniques

Interactions between contact surfaces were established in the FE model. The interactions had many features that are necessary for the solution's appropriate convergence and were determined by the physical relationship between its components [3].

III. RESULTS AND DISCUSSION

The distributions of stresses and displacements were studied to properly exploit and develop the results of 3D modeling. Figure 5 shows the collected results of stresses and their vertical distribution from the FE model analysis used in this study for case 1, while Figure 6 shows the vertical displacement distribution within the pavement layers. Figures 7-10 show the collected results of stresses and vertical displacement distribution within pavement layers for cases 2 and 3.

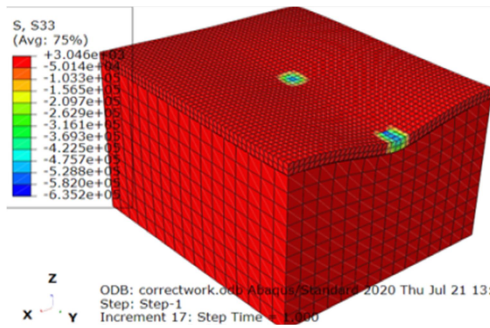


Fig. 5. Stress distribution within pavement layers, case 1.

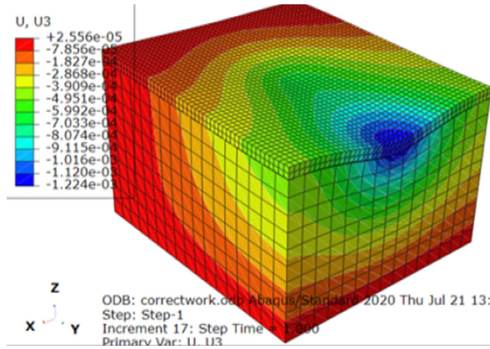


Fig. 6. Vertical displacement distribution within pavement layers, case 1.

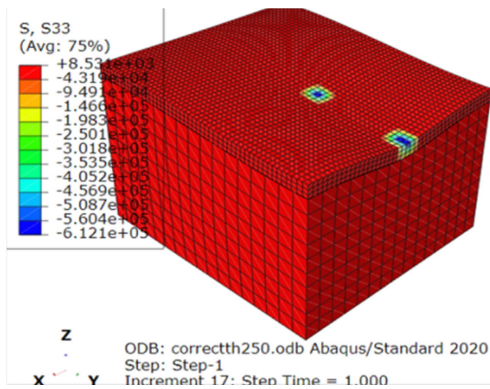


Fig. 7. Stress distribution within pavement layers, case 2.

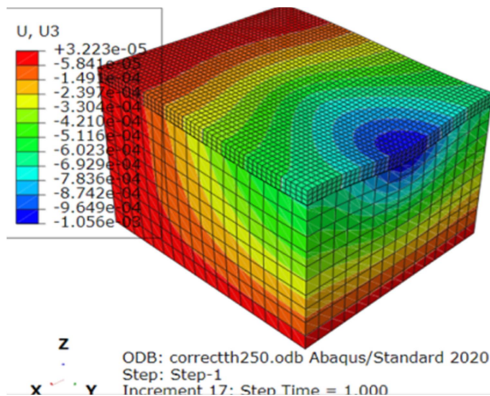


Fig. 8. Vertical displacement distribution within pavement layers, case 2.

concrete slab layer under the tire print, which is about 75% of the applied pressure. This was reduced to 190kPa at the top of the subgrade layer, which is about 28% of the applied pressure. In case 2, vertical stress increased to 598kPa at the top of the concrete slab layer, which is approximately 87% of the applied pressure, and reduced to 163kPa at the top of the subgrade layer, which is approximately 24% of the applied pressure. In case 3, vertical stress increased to 610kPa and 150kPa at the top of the concrete slab and subgrade layers (approximately 88% and 22% of the applied pressure) respectively.

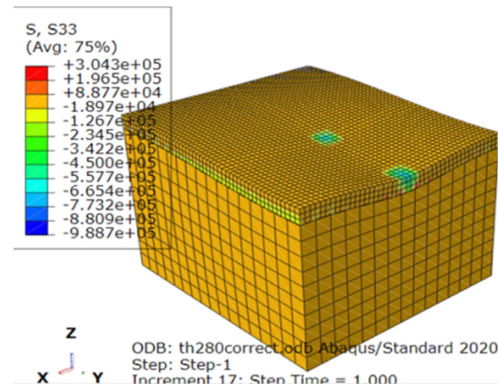


Fig. 9. Stress distribution within pavement layers, case 3.

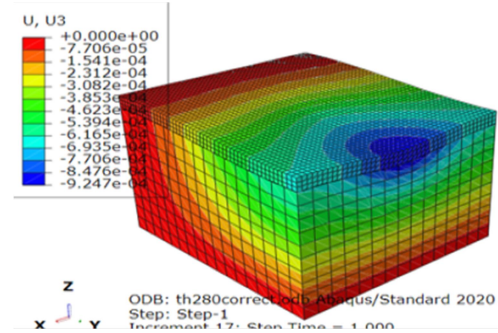


Fig. 10. Vertical displacement distribution within pavement layers, case 3.

TABLE III. STRESS LEVELS BETWEEN THE INTERFACED LAYERS

Layer name	Vertical Stress (σ_{33}), Pa		
	Case 1	Case 2	Case 3
Top of concrete slab layer	519652	598887	610052
Top of subgrade	190376	163143	150807

The results of this study indicate that the stress levels at the top of the concrete slab layer increased by approximately 88% when the thickness of this layer increased from 20 to 28cm, while the stress levels at the top of the subgrade layer reduced by approximately 21%. Figure 11 illustrates how the stress level increased with the increasing thickness of the concrete slab layer. Additionally, as the thickness of the concrete slab layer increases, the vertical stresses below the tire print at shallow depths vary slightly. However, at large horizontal distances and depths, the variation is negligible.

Figure 12 shows the vertical displacement along with the horizontal distance for all cases on top of the concrete slab layer under the center of the inner wheel. The vertical displacement in the middle of the horizontal distance under the

Table III shows the values of vertical stresses (σ_{33}) in the pavement system when applying a pressure of 690kPa. In case 1, vertical stress of 519kPa was concentrated on the top of the

tire print decreased by 14%, 12%, and 24% when the concrete slab layer increased from 20 to 25cm, 25 to 28cm, and 20 to 28cm respectively. However, the vertical displacement at the edge of the concrete slab layer increased by about 26% when the thickness of this layer increased from 20 to 28 cm.

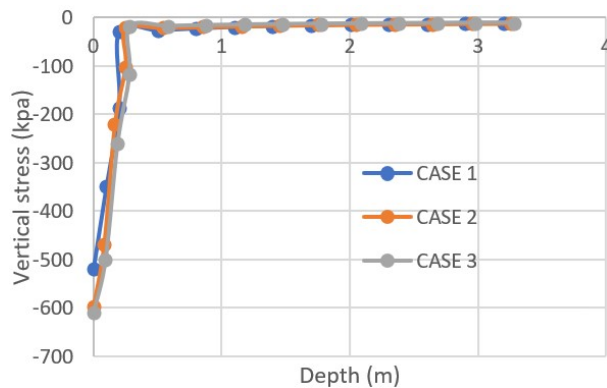


Fig. 11. Vertical stress vs depth.

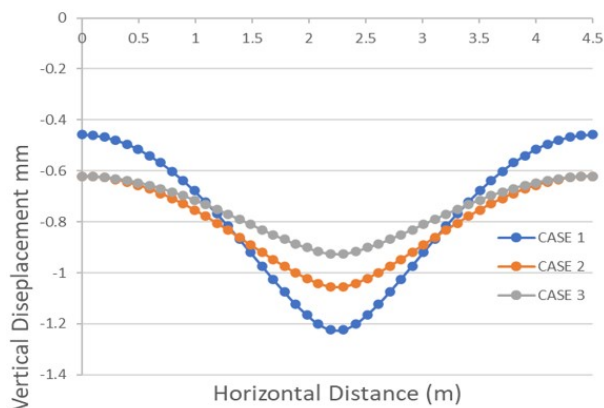


Fig. 12. Vertical displacement on the top of the concrete slab layer.

IV. CONCLUSION

The main conclusions drawn from on the results of this study are:

- The percentage of deformation in the middle of the horizontal distance under the tire print decreases by 14%, 12%, and 24% as the thickness increases from 20 to 25cm, 25 to 28cm, and 20 to 28cm respectively. This indicates that the concrete slab layer is mainly responsible for this reduction in deformation in the pavement structure.
- For concrete slab layer thicknesses of 20, 25, and 28cm, the vertical stress at the top of the concrete slab layer is 519, 598, and 610kPa respectively, and it reduces to 190, 163, and 150kPa on the top of the subgrade layer, which is equivalent to approximately 28%, 24%, and 22% of the applied stress at the top. Since the stresses in the layer under the concrete slab layer decrease as the thickness of the concrete slab layer increases, the stresses above the subgrade therefore decrease.
- The maximum value of vertical stress is 610.052Pa at the top of the concrete slab layer when the concrete slab layer

is 28cm, while the minimum vertical stress is 100.152 at the top of the subgrade layer when the concrete slab layer is 25cm.

- The analysis clearly shows that the vertical stress at the top of the concrete slab layer increases as the vertical depth of the concrete slab layer increases.

REFERENCES

- [1] F. M. H. López, E. T. Piusseaut, E. A. R. Veliz, and C. A. R. Morfa, "3D-FE of jointed plain concrete pavement over continuum elastic foundation to obtain the edge stress," *Revista de la Construcción - Journal of Construction*, vol. 19, no. 1, pp. 5–18, Apr. 2020, <https://doi.org/10.7764/RDLC.19.1.5-18>.
- [2] M. Zokaei, M. Fakhri, and S. Rahiminezhad, "A Parametric Study of Jointed Plain Concrete Pavement Using Finite Element Modeling," *Modern Applied Science*, vol. 11, no. 11, pp. 75–84, Oct. 2017, <https://doi.org/10.5539/mas.v11n11p75>.
- [3] Y. H. Huang, *Pavement Analysis and Design*, 2nd ed. Upper Saddle River, NJ, USA: Pearson Education, 2004.
- [4] M. Zdiri, N. Abriak, J. Neji, and M. B. Ouezdou, "Modelling of the Stresses and Strains Distribution in an RCC Pavement Using the Computer Code 'Abaqus,'" *Electronic Journal of Structural Engineering*, vol. 9, pp. 37–44, Jun. 2009, <https://doi.org/10.56748/ejse.9116>.
- [5] A. S. Mahdi and S. D. Mohammed, "Experimental and Numerical Analysis of Bubbles Distribution Influence in BubbleDeck Slab under Harmonic Load Effect," *Engineering, Technology & Applied Science Research*, vol. 11, no. 1, pp. 6645–6649, Feb. 2021, <https://doi.org/10.48084/etasr.3963>.
- [6] A. A. Abdulhussein and M. H. Al-Sherrawi, "Experimental and Numerical Analysis of the Punching Shear Resistance Strengthening of Concrete Flat Plates by Steel Collars," *Engineering, Technology & Applied Science Research*, vol. 11, no. 6, pp. 7853–7860, Dec. 2021, <https://doi.org/10.48084/etasr.4497>.
- [7] W. Uddin, R. M. Hackett, A. Joseph, Z. Pan, and A. B. Crawley, "Three-Dimensional Finite-Element Analysis of Jointed Concrete Pavement with Discontinuities," *Transportation Research Record*, vol. 1482, pp. 26–32, 1995.
- [8] M. R. K. Manesh, M. M. S. Babaki, A. P. Tavandasthi, "Examining the Effect of Weight and the Arrangement of Aircrafts' Wheels on Roller-Compacted Concrete (RCC) Pavement Design of Runways Using Finite Element Method," *Current World Environment*, vol. 10, Special Issue 1, Apr. 2015.
- [9] Sii, How Bing (Perry), "Three-dimensional finite element analysis of concrete pavement on weak foundation," Ph.D. dissertation, Griffith University, Queensland, Australia, 2015.
- [10] M. a. S. Hadi and M. H. Al-Sherrawi, "The Influence of Base Layer Thickness in Flexible Pavements," *Engineering, Technology & Applied Science Research*, vol. 11, no. 6, pp. 7904–7909, Dec. 2021, <https://doi.org/10.48084/etasr.4573>.
- [11] M. Rahman and N. Murshed, "Sensitivity of Rigid Pavement Responses to Pavement Layer Thickness Due to Wheel Load: A Nonlinear Finite Element Study," *Trends in Transport Engineering and Applications*, vol. 1, no. 1, pp. 1–10, 2014.